# Physicochemical Studies of Ni-, Co-, and Pt- Promoted MoVNbOx Catalysts Synthesised by Impregnation Method

**M.S. WONG[1], R. IRMAWATI[1,2]\*, H. ABBASTABAR AHANGAR[1,3],**
**Y.H. TAUFIQ YAP[1,2], Y.P. TAN[1,2] and E.N. MUHAMAD[1,2]**

[1] Centre of Excellence for Catalysis Science and Technology ,
[2] Department of Chemistry, Faculty of Science, Universiti Putra Malaysia,
43400 UPM Serdang, Selangor, Malaysia.
[3]Materials Science and Engineering Department, Islamic Azad University,
Najafabad Branch, Najafabad 85141-43131, Iran.

## ABSTRACT

Ni-, Co-, and Pt- promoted MoVNbOx mixed metal oxide catalysts were prepared by impregnation method. The physicochemical properties of the catalysts showed that the BET surface area of the promoted catalysts was lower when compared to the unpromoted catalysts due to the filling of open pores by the promoters. X-ray diffraction (XRD) analysis indicated that the main reflections were consistent with the tetragonal rutile structure. Three crystalline phases of $(V_{0.07}Mo_{0.93})_5O_{14}$, $(Nb_{0.09}Mo_{0.91})O_{2.80}$, and $Mo_4O_{11}$ could also be observed. Induced Coupled Plasma-Optical Emission Spectroscopy (ICP-OES) displayed the loss of metal promoters, mainly due to sublimation during calcination with Pt-MoVNbOx. Temperature Programmed Reduction ($H_2$-TPR) exhibited high reducibility for samples loaded with $10^{-3}$ wt% promoter. The level of reduction declines with increased loads, suggesting a stronger oxygen bond in the promoted metal oxide catalysts.

**Keywords:** propane oxidation; acrylic acid; MoVNbOx catalysts; oxidative dehydrogenation; tetragonal rutile; $H_2$-TPR.

## INTRODUCTION

There have been recent reports of the use of propane instead of propylene as the starting material for the production acrylic acid [1,2]. Propane's lower prices and abundance make it an attractive and important commodity in the petrochemical industry. The drawback is that propane is much more inactive if compared to propylene due to its saturated nature and therefore its lack of π electrons for reactions. However, Ushikubo *et al.* [3] successfully developed MoVTeNbOx catalysts with an orthorhombic structure that has excellent activity and selectivity for partial oxidation of propane to acrylic acid at a moderate temperature. The catalysts were prepared using a hydrothermal method and were calcined at 873 K in nitrogen for 2 hours to achieve the desired phase. Other researchers have embarked on studies of MoVNbOx catalysts with a tetragonal rutile structure, which exhibit very good activity as well [4,5,6,7,8,9]. Tellurium is no longer used as catalyst is due to its tendency to sublime during

calcination. With its melting point of around 723-748 K, an effective calcination temperature of 873 K would vaporize Te from the catalyst's surface. The loss of Te would reduce the acrylic acid's selectivity needed in the formation and release acrylic acid from the surface of the catalyst [2]. López-Medina *et al.* [10] produced a nanoscale tetragonal rutile MoVNb alumina-supported catalyst which has a conversion rate of about 10% for propane and 70% selectivity to acrylic acid by using $Mo_7V_2Nb_1$. The oxidative dehydrogenation (ODH) of propane to propylene is the rate-determining step for the partial oxidation of propane to acrylic acid [11,12,13,14]. The benefit of rutile structures in MoVNbOx as opposed to the orthorhombic structures in MoVTeNbOx is their ability to host a large amount of cationic vacancies, which encourages the H-abstraction properties of $V^{4+}$ [15], the rate-determining step of the propane reaction. Vacancies are formed due to either the excess positive charges generated by oxidation of $V^{3+}$ - $V^{4+}$ and $V^{5+}$, or the incorporation of altervalent cations in the rutile lattice. Additionally, Mo and V are responsible for activating propane while Nb helps to stabilize the desired catalyst structure in the redox cycle and permits the catalyst to return to its original state. In order to increase the rate of ODH, MoVNbOx is promoted by Ni[16,17], Co[18,19] or Pt [20] since they are good dehydrogenation agents.

In this study, the MoVNbOx catalysts were prepared by slurry. The catalysts were later promoted by Ni, Co and Pt and their physicochemical characteristics are discussed.

### Catalyst Preparation

The MoVNbOx catalysts in the metal atomic ratio of Mo:V:Nb = 1:0.25:0.12 [21,22] were prepared by dissolving 6.76 g of ammonium heptamolybdate (Merck), 1.11 g of ammonium metavanadate (BDH), and 1.38 g of ammonium niobium oxalate (Aldrich), in 150 ml of deionised water. The solutions were mixed and heated to 353 K for 60 min while stirring. The mixture was then dried using a rotatory evaporator at 353 K and the precipitate was ground into powder. The powder was calcined at 873 K in a nitrogen gas flow for 2 hours.

Amounts of $10^{-3}$ wt%, $10^{-2}$ wt%, $10^{-1}$ wt%, 1 wt%, 3 wt%, and 5 wt% of nickel nitrate hexahydrate (Sigma-Aldrich) and cobalt(II) nitrate hexahydrate (Acros Organics); and $10^{-3}$ wt%, $10^{-2}$ wt%, $10^{-1}$ wt% and 1 wt% of trans-platinum(II) diamine dichloride (Sigma-Aldrich) were impregnated onto the prepared solid catalysts, respectively. The promoted MoVNbOx catalysts were oven-dried at 353 K. The dried promoted MoVNbOx was ground into powder and calcined at 873 K in a nitrogen gas flow for 2 hours. The obtained promoted MoVNbOx catalysts were labelled as -3*A*, -2*A*, -1*A*, 1*A*, 3*A*, and 5*A* in accordance to the amount of promoters of $10^{-3}$ wt%, $10^{-2}$ wt%, $10^{-1}$ wt%, 1 wt%, 3 wt% to 5 wt%, whereas *A* is referred to Ni, Co or Pt.

### Characterisation of samples

X-ray diffraction (XRD) were used to identify the sample crystalline plane. This analysis was performed by a Shimadzu Model XRD-6000 diffractometer. Diffraction patterns were produced by employing $CuK_\alpha$ radiation at 30 mA and 40 kV, generated by a Phillips glass X-ray diffraction tube with a broad focus of 2.7 kW at ambient temperature. The scanning rate was 4.000° $min^{-1}$ with a 2θ range of 10° to 77°.

The specific surface area of the samples was measured by using BELSorp Mini II. 0.2 – 0.5 g of calcined samples was degassed prior to analysis. The surface area of the samples was determined by calculating the amount of adsorbed nitrogen based on the Brunauer-Emmett-Teller method.

Induced Coupled Plasma- Optical Emission Spectroscopy (ICP-OES) was used to determine the elemental composition of the catalysts. Inductively Coupled Optima 2000 was the instrument used for this purpose. About 0.03g of powdered catalyst was dissolved in 5 ml of $H_2SO_4$ with slow heating. The solution was transferred into a 250 ml volumetric flask and topped up with deionised water.

$H_2$ temperature programmed reduction ($H_2$-TPR) was performed by Thermo Finnigan TPDRO 1100 Series. Samples underwent pretreatment by heating in $N_2$ gas at 473 K. Reduction analysis was preceded by temperature programming from 323 to 1173 K by using 5 % hydrogen in argon at a heating rate of 10 K/min.

## RESULTS AND DISCUSSION

### X-ray Diffractogram

The XRD patterns of MoVNbOx and promoted samples are shown in Fig. 1. All of the samples demonstrate similar diffraction patterns, which are found to be consistent with tetragonal rutile MoV phases at $2\theta$ = 25.0°, 26.4°, 37.1°, and 54.0°. The results are consistent with observations made by López-Medina *et al.* [10] in their work on alumina-supported MoVNbOx catalysts, although the overlapping of those peaks with $MoO_2$ and $\gamma$-$Al_2O_3$ could not be denied. Additionally, other crystalline phases such as $(V_{0.07}Mo_{0.93})_5O_{14}$ (JCPDS 00-031-1437) and $(Nb_{0.09}Mo_{0.91})O_{2.80}$ (JCPDS 00-027-1310) phases at $2\theta$ = 12.3°, 16.4°, 22.2°, 23.4°, 25.0°, 26.1°, 27.6°, 31.6°, 32.7°, 33.6°, and 38.9°; and $Mo_4O_{11}$ (JCPDS 01-089-5109) with $2\theta$ = 22.2°, 23,3°, 26.1°, 27.6°, 31.5°, 32.9°, 33.9°, 37.0°, 39.2°, 45.6°, 49.0°, 51.1°, 54.0°, 56.4°, and 59.1° were also observed. The crystallinity of mixed oxides increased with the addition of promoters as
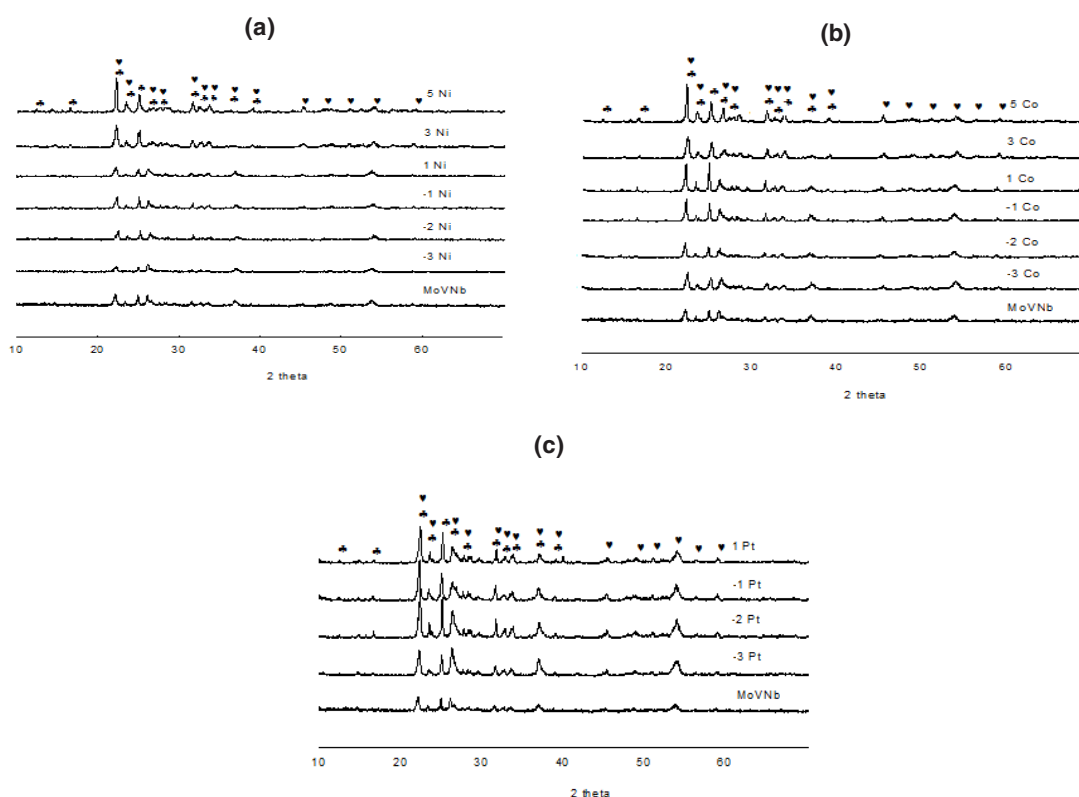


**(a)**

**(b)**

**(c)**

**Fig. 1: X-ray diffraction of (a) Ni-promoted (b) Co-promoted (c) Pt-promoted MoVNb mixed oxide catalysts, ♣ - $(V_{0.07}Mo_{0.93})_5O_{14}$ and $(Nb_{0.09}Mo_{0.91})O_{2.80}$ , ♥- $Mo_4O_{11}$**

evidenced by the sharper and more intense peaks for Co- and Pt- promoted samples. In Ni-promoted samples, the peaks became more intense when 5 wt% of Ni was added to MoVNbOx. The promoters demonstrated their function as a structural promoter which affects the crystalline structure formation [23].

### BET Surface Area

The BET specific surface area values, $S_{BET,}$ of MoVNbOx and promoted-MoVNbOx samples are listed in Table 1. The surface area of unpromoted MoVNb is 8.8 m²/g. The $S_{BET}$ values decreased when the catalysts were added with Ni, Co and Pt promoters. $S_{BET}$ values continued to decrease the addition of more promoters. This trend was observed in every promoted sample. The decrease in $S_{BET}$ values in all promoted samples is due to the presence of metals on the voids and open pores of

the catalysts. Metals cover the open pores and lower the catalyst's surface area.

## Chemical Composition

The elemental composition of catalysts was determined by Induced Coupled Plasma-Optical Emission Spectroscopy (ICP-OES) and the data can be seen in Table 1. The theoretical atomic molar ratio of unpromoted $Mo_1V_{0.25}Nb_{0.12}$ was found to be similar to the experimental value, which is 1:0.24:0.13. The chemical composition of the promoters on the catalysts was slightly lower than the theoretical values. This is likely due to sublimation of the metals during calcinations, which was especially evidenced in the Pt-promoted catalyst where none of Pt could be detected in any of the samples. Pt undergoes sublimation either in its elemental form or as reacted species during

**Table 1. The physicochemical properties of catalysts.**

| Catalyst | $S_{BET}$ (m²/g) | Chemical composition[a] | |
| --- | --- | --- | --- |
| | | Theoretical Value | Experimental value |
| MoVNbOx | 8.8 | Atomic ratio 1:0.25:0.12 | 1:0.24:0.13 |
| -3Ni | 6.4 | 0.001 wt% Ni | nd |
| -2Ni | 5.1 | 0.010 wt% Ni | 0.010 wt% Ni |
| -1Ni | 4.3 | 0.100 wt% Ni | 0.080 wt% Ni |
| 1Ni | 4.6 | 1.000 wt% Ni | 0.839 wt% Ni |
| 3Ni | 4.2 | 3.000 wt% Ni | 2.732 wt% Ni |
| 5Ni | 2.3 | 5.000 wt% Ni | 4.887 wt% Ni |
| -3Co | 4.4 | 0.001 wt% Co | nd |
| -2Co | 3.7 | 0.010 wt% Co | 0.003 wt% Co |
| -1Co | 3.3 | 0.100 wt% Co | 0.078 wt% Co |
| 1Co | 3.7 | 1.000 wt% Co | 0.520 wt% Co |
| 3Co | 3.3 | 3.000 wt% Co | 2.508 wt% Co |
| 5Co | 1.6 | 5.000 wt% Co | 4.023 wt% Co |
| -3Pt | 5.6 | 0.001 wt% Pt | nd |
| -2Pt | 5.7 | 0.010 wt% Pt | nd |
| -1Pt | 5.8 | 0.100 wt% Pt | nd |
| 1Pt | 5.2 | 1.000 wt% Pt | nd |

[a]Chemical composition of each element in samples determined by Induced Coupled Plasma- Optical Emission Spectroscopy (ICP-OES);     nd: not determined

calcinations [24,25]. The reacted species such as $PtO_2$ has a melting point around 723 K, which would allow it to undergo sublimation during calcinations at 873 K. Additionally, the calcinations were under nitrogen flow where Pt could be carried away in vapor form. This observation is similar to MoVTeNbOx catalysts where a small atomic percentage of Te was found when samples were calcined in $N_2$ at 873 K [2].

## H$_2$-TPR analysis

Temperature programmed reduction in hydrogen (H$_2$-TPR) was performed to study the reducibility of the metal oxide catalysts when exposed to hydrogen, a reducing gas. The reaction between $H_2$ with the oxygen species adsorbed on/in the surface of the catalyst can be represented as:

$$H_{2(g)} \; + \; O_s \rightarrow H_2O_{(g)} \; + \; \uparrow$$
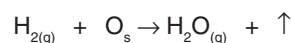
where (g), s and $\uparrow$ represent gaseous, surface and vacant sites.

In the TPR analysis, the hydrogen gas interacts with the surface oxygen species, $O^-$ and forms water molecules which are desorbed from the catalyst's surface, leaving behind vacant sites[26].
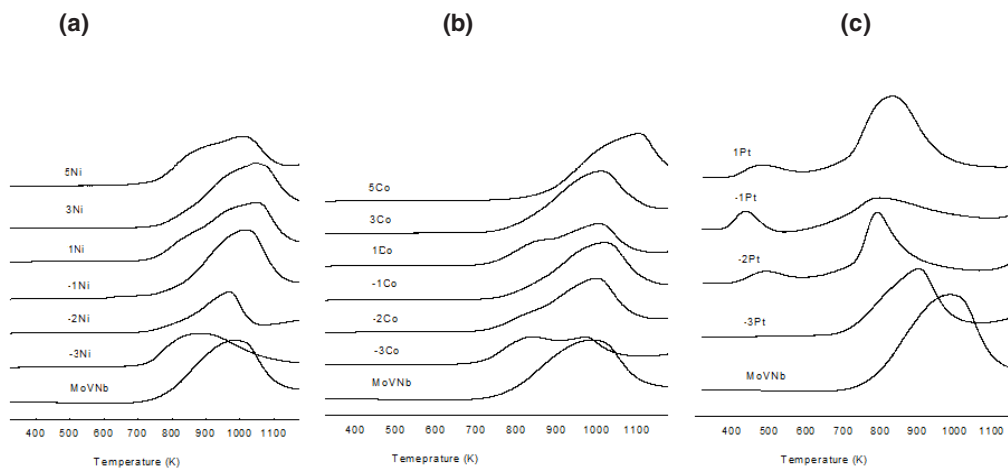
(a)                              (b)                              (c)



**Fig. 2: H$_2$-TPR profile of (a) Ni-promoted (b) Co-promoted
(c) Pt-promoted MoVNb mixed oxide catalysts.**

The reduction profiles of the catalysts can be seen in Fig. 2. For the unpromoted MoVNbOx, the reduction profile exhibited a broad desorption peak between 700 and 1200 K with a reduction peak of 982 K. Jiang *et al.* [27] reported that the reduction profile of pure MO$_n$ was at 948 K and 995 K and pure VO$_n$ was at of 913 K and 943 K. It is believed that Mo and V species undergo stepwise reductions as follows, Mo$^{6+}$ → Mo$^{4+}$ and Mo$^{4+}$ → Mo$^0$. Meanwhile, according to Pereira *et al.* [28], reduction at around 1243 K indicates the reduction of Nb$^{5+}$ to Nb$^{4+}$. Therefore, the reduction peak observed in this work at the peak maximum of 982 K in MoVNbOx catalyst could be ascribed to the reduction of V$_2$O$_5$ → VO$_2$[29], MoO$_3$ → MoO$_2$[27,29], and Nb$_2$O$_5$ → NbO$_2$[28].

For the promoted MoVNbOx catalysts, the H$_2$-TPR a lower peak maximum profile for 10$^{-3}$ wt% loading sample was indicated as compared to the unpromoted sample. Beyond this weight percentage, except for Pt-loaded samples, the peak maximum is higher than the unpromoted samples. This observation could be due to well-dispersed metal particles on the catalyst's surface, which have weaker bonds with the oxygen species. The promoted catalyst is more reducible when compared to the unpromoted samples. With increased loading, stronger bonds form, leading to higher reduction peak maxima as is observed in the samples.

The reduction profile of Ni-MoVNbOx is possibly due to the reduction of VO$_n$, MoO$_n$, NbO$_n$ and also from NiO$_2$ → Ni[30]. The reduction profile for Co-MoVNbOx can be attributed to the reduction of V$_2$O$_5$ → VO$_2$[29], MoO$_3$ → MoO$_2$[27,29], and Nb$_2$O$_5$ → NbO$_2$[28]. One noticeable difference between these profiles when compared to the Ni-promoted samples is the appearance of overlapping two peak maxima which is clearly seen in -3Co. The appearance of two peaks was expected and is due to the stepwise reduction of Co. According to Liu *et al.* [31], the first reduction peak represents the reduction of Co$^{3+}$ to Co$^{2+}$ which then experiences a structural change to CoO and the second reduction peak indicates a change to Co metal. However, the spectra for the remaining Co-promoted samples did not produce a clear double peak due to the uneven distribution of Co on the catalyst's surface.

The reduction profiles of the Pt-MoVNbOx samples produced two distinct peak maxima at the low temperature range of 435 K – 480 K and at the high temperature range of 792 K – 832 K. The reduction profile at the higher temperature is due to the decomposition of PtO$_2$ to PtO$_x$ or metal Pt. This is similar to the observation by Liang *et al.* [32] who discovered the same reduction at around 673 K. They added that the decomposition temperature is based on the sample's particle size and properties. It is believed that all the Pt species are

reduced to $PtO_x$ and Pt metal in the high temperature range. The lower temperature peak maxima could be due to the weak oxygen bonds of the finely dispersed Pt species.

## CONCLUSION

The unpromoted MoVNbOx and Ni-, Co-, and Pt-promoted MoVNbOx catalysts present similar tetragonal rutile crystalline phases, which is desirable for the conversion of propane to acrylic acid.  The crystallinity of catalysts increased with the loading of the promoter, thus indicating the positive role of Ni, Co and Pt.   Although a small amount of the metal might be lost during calcination, its presence on the catalyst's surface has a strong effect on the catalyst's reducibility by forming oxide bonds with the metal oxide. The Ni-, Co- and Pt-promoted MoVNbOx catalysts are more reducible, at least for the lowest loading sample $10^{-3}$ wt%, when compared to those with higher loads.

## REFERENCES

1.      Lin M M, *Applied Catalysis a-General,* **250:** 287-303 (2003).
2.      Lin M M, *Applied Catalysis a-General,* **250:** 305-318 (2003).
3.      Ushikubo T, Nakamura H, Koyasu Y, Wajiki S,  pp. US Patent 5380933A to Mitsubishi Kasei Corporation (1995).
4.      Ivars F, Solsona B, Soriano M, López Nieto J, *Topics in Catalysis,*  **50:** 74-81 (2008).
5.      Botella P, López Nieto J M, Dejoz A, Vázquez M I, Martínez-Arias A, *Catalysis Today,* **78:** 507-512 (2003).
6.      Botella P, Concepción P, López Nieto J M, Solsona B, *Catalysis Letters,* **89:** 249-253 (2003).
7.      Ivars F, Solsona B, Botella P, Soriano M D, López Nieto J M, *Catalysis Today,* **141:** 294-299.(2009)
8.      Ueda W, Endo Y, Watanabe N, *Topics in Catalysis,* **38:** 261-268 (2006).
9.      Chaudhari C S, Sable S S, Gurav H, Kelkar A A, Rane V H, *Journal of Natural Gas Chemistry,* **19:** 593-599 (2010).
10.     López-Medina R, Fierro J L G, Guerrero-Pérez M O, Bañares M A, *Applied Catalysis A: General,* **375:** 55-62 (2010).
11.     Meunier F C, Yasmeen A, Ross J R H, *Catalysis Today,*   33-42 (1997).
12.     Kondratenko E V, Baerns M, *Applied Catalysis A: General,* **222:** 133-143 (2001).
13.     Fukudome K, Ikenaga N-o, Miyake T, Suzuki T, *Catalysis Science & Technology,* **1:** 987-998 (2011).
14.     Cavani F, Trifirò F, *Catalysis Today,* **24:** 307-313 (1995).
15.     Ballarini N, Cavani F, Di Memmo S, Zappoli F, Marion P, *Catalysis Today,* **141:** 264-270 (2009).
16.     Stern D L, Grasselli R K, Mechanistic aspects of propane oxidation over Ni-Co-molybdate catalysts, in: S.T.O.A.M.G. R.K. Grasselli, J.E. Lyons (Eds.), *Studies in Surface Science and Catalysis,* Elsevier, pp. 357-365 (1997).
17.     AbdelDayem H M, Ruiz P, Enhancement of the Catalytic Performance of NiMoO4 and Modification of the Kinetic parameters of Oxidative Dehydrogenation of Propane over NiMoO4/Sb2O4 Biphasic Catalyst by Oxygen spillover, in: A. Guerrero-Ruiz, I. Rodriguez-Ramos (Eds.), *Studies in Surface Science and Catalysis,* Elsevier,  pp. 363-370 (2001).
18.     Palacio L A, Echavarría A, Sierra L, Lombardo E A, *Catalysis Today,* **107-108:** 338-345 (2005).
19.     Ueda W, Yoon Y-S, Lee K-H, Moro-oka Y, *Korean Journal of Chemical Engineering,* **14:** 474-478 (1997).
20.     Vajda S, Pellin M J, Greeley J P, Marshall C L, Curtiss L A, Ballentine G A, Elam J W, Catillon-Mucherie S, Redfern P C, Mehmood F, Zapol P, *Nat Mater,* **8:** 213-216 (2009).
21.     Linke D, Wolf D, Baerns M, Timpe O, Schlogl R, Zeyss S, Dingerdissen U, *Journal of Catalysis,* **205:** 16-31 (2002).
22.     Kum S S, Jo B Y, Moon S H, *Applied Catalysis A: General,* **365:** 79-87 (2009).

23.   Idris R, Hamid S B A, *The Malaysian Journal of Analytical Sciences,* **13(1):** 86-93 (2009).
24.   Petkovic L M, Ginosar D M, Rollins H W, Burch K C, Pinhero P J, Farrell H H, *Applied Catalysis A: General,* **338:** 27-36 (2008).
25.   Holleman A F, Wiberg E, Wiberg N, *Inorganic Chemistry,* Academic Press, San Diego (2001).
26.   Irmawati R, Noorfarizan Nasriah M N, Taufiq-Yap Y H, Abdul Hamid S B, *Catalysis Today,* **93-95:** 701-709 (2004).
27.   Jiang H C, Lu W M, Wan H L, *Journal of Molecular Catalysis a-Chemical,* **208:** 213-217 (2004).

28.   Pereira E B, Pereira M M, Lam Y L, Perez C A C, Schmal M, *Applied Catalysis A: General,* **197:** 99-106 (2000).
29.   Guan J, Song K, Xu H, Wang Z, Ma Y, Shang F, Kan Q, *Catalysis Communications,* **10:** 528-532 (2009).
30.   Abu Bakar N H H, Bettahar M M, Abu Bakar M, Monteverdi S, Ismail J, Alnot M, *Journal of Catalysis,* **265:** 63-71 (2009).
31.   Liu Q, Wang L-C, Chen M, Cao Y, He H-Y, Fan K-N, *Journal of Catalysis,* **263:** 104-113 (2009).
32.   Liang H, Zhang Y, Liu Y, *Journal of Natural Gas Chemistry,* **17:** 403-408 (2008).